Hydrogen Molecule Clusters†

Matthew Carmichael, Kimberly Chenoweth, and Clifford E. Dykstra*

Department of Chemistry, Indiana University-Purdue University Indianapolis, 402 North Blackford Street, Indianapolis, Indiana 46202

Received: October 23, 2003; In Final Form: January 2, 2004

Ab initio calculations at the MP2 and coupled cluster levels have been performed for small clusters of hydrogen molecules. A concise model interaction potential was constructed on the basis of ab initio potential surface points for the dimer and on comparison with ab initio results for the trimer and tetramer. The model was used to investigate key features of cluster growth, starting with the aggregation energies for clusters with up to 10 molecules. Fully anharmonic zero-point vibrational energies were evaluated for these clusters and were found to be a sizable fraction of the well depth for small clusters. Calculations on larger clusters were used to follow the approach to regular structures in large aggregations, the energetics of cluster growth, and the internal rotation potential for hydrogen molecules embedded in a large cluster. It was found that the essentially free rotation involves concerted reorientation of hydrogen molecules in the first surrounding shell.

Introduction

Hydrogen's use or potential use as a fuel or an energy storage material for automobiles and other devices draws attention to technological problems not only of its generation and combustion but also of its storage and containment.[1] The latter issues might require full or at least deeper understanding of the weak, noncovalent bonding interactions among hydrogen molecules, between hydrogen and molecules that might be seeded in bulk hydrogen, and between hydrogen and containment materials. Calculational treatments may prove an efficient means for an initial evaluation of certain technological issues while also offering insights to physical phenomena of intermolecular interactions with hydrogen molecules. For instance, there have already been simulations and connected experiments for certain very interesting features of the absorption of H_2 in amorphous water ice,[2−4] X-ray study of H_2-H_2O clathrates,[5] and simulations of molecular hydrogen in carbon nanotubules.[6] In fact, the latter of these studies directly addresses several of the technological issues such as storage capacity of carbon nanotubules for which an upper limit value of ∼7.7 wt % was found. Even if, in the end, the technological developments do not evolve from basic interaction information, there are potentially interesting cluster phenomena to be explored for such a low-mass molecule. The first part of that exploration involves the interaction of hydrogen molecules with each other, and an essential step is developing a model potential designed for small to moderately large clusters and extensive simulations.

The well depth for the weak interaction potential of two hydrogen molecules is several times that of He_2, yet it is still very much less than the well depth for almost any pair of closed-shell neutral molecules that contain at least one element more massive than hydrogen. The H_2-H_2 interaction is of special interest among weakly bound systems because both of the two primary sources of attraction, dispersion and permanent electrical moments, have sizable roles. For instance, using the values we have obtained here, the quadrupole−quadrupole interaction energy of the dimer at its equilibrium structure is roughly 60% of the well depth and the dispersion energy is around 150% of the well depth. Of course, other effects are partly offsetting these attractive elements to make for the very shallow well.

The shallowness of the pair interaction of hydrogen molecules calls for potential surface evaluations that can carefully reflect the ultimate applications of the surface and the desired accuracy. Hence, for the first objective of this study, that of ab initio calculation of H_2-H_2 potential surface points, different basis sets and correlation treatments were employed. While a number of studies[7−19] have found pair−pair potentials or potential surface data for $(H_2)_2$, we have followed a more focused or specific aim, that of achieving a model potential for the well region or basically for the parts of the interaction surface sampled most by ground state vibrational excursions of the weakly bound cluster. This means that we have obtained ab initio potential surface points mostly in regions where the interaction energy is at or below the zero-point energy of the dimer. With this focus we hope to have a model of sufficient reliability to obtain key structural and energetic information for clusters of many hydrogen molecules. Our ab initio calculations for $(H_2)_3$ and $(H_2)_4$ show that the model achieved a level of accuracy that matches the reliability for $(H_2)_2$. Among many of the prior studies of the H_2-H_2 interaction potential has been the objective of simulating scattering cross sections or other phenomena that require good accuracy on or along the close-in repulsive walls of the potential surface. As a more global surface problem than our objective, that will tend to require more complicated mathematical forms for a model potential. Our specific focus, then, has an intended benefit of being easily workable in application to a hundred or more molecules, not only the dimer, and workable for dynamical simulations requiring numerous potential evaluations. We report one such evaluation here, one that involved on the order of 10^{11} evaluations. Furthermore, in future work, we expect to take advantage of this potential for mixed clusters, and that is facilitated by the concise and partly transferable form of the model used here. At the same time, this model is not intended to match the highest accuracy, global surface representations for $(H_2)_2$ that have been achieved to date.

† Part of the special issue "Fritz Schaefer Festschrift".

10.1021/jp037209u CCC: $27.50
Published on Web 02/24/2004

TABLE 1: Calculated Equilibrium Properties of H_2[a]

	R_{eq} (Å)	Q_{xx}	α_{xx}	$\alpha_{zz} = \alpha_{yy}$
		cc-pVTZ Basis		
SCF	0.734	0.9677	6.606	2.620
MP2	0.737	0.9593	6.556	2.593
full-CI	0.743	0.9419	6.537	2.594
		aug-cc-pVTZ Basis		
SCF	0.734	1.0035	6.473	4.645
MP2	0.737	0.9841	6.454	4.618
full-CI	0.743	0.9253	6.438	4.614
		d-aug-cc-pVTZ Basis		
SCF	0.734	0.9980	6.481	4.637
MP2	0.737	0.9786	6.462	4.590
full-CI	0.743	0.9203	6.430	4.612

[a] Except for the equilibrium bond length, properties are in au and were evaluated at the full-CI equilibrium distance of 0.743 Å. The quadrupole moments are in traceless form, and hence, $Q_{yy} = Q_{zz} = -Q_{xx}/2$ (1 au = 1.34504 D Å).

It is interesting to note that the interaction of two H_2 molecules had an early place in the development and application of large-scale quantum mechanical methods. It was in 1972 that Bender and Schaefer[20] performed calculations on colinear $(H_2)_2$ that pushed the limits of existing configuration interaction methodology. Furthermore, similarly large-scale calculations on the isoelectronic He_2 dimer[21] provided a potential that helped guide later efforts at building $(H_2)_2$ potentials.[9]

The potential surface for the dimer displays the orientational features of interacting quadrupoles primarily, with the equilibrium structure being a T-shaped arrangement of the two molecules. The other preferred arrangement of two quadrupoles, a slipped or offset parallel structure, is almost as energetically favorable for $(H_2)_2$. Furthermore, there is essentially free rotation of the molecules,[22,23] and this is also known to be the case for the solid.[24] The structure of the trimer of hydrogen molecules is cyclic, and the stabilization energy of the trimer is very close to the sum of pairwise interactions of the three molecules. The structures and stabilities of larger clusters offer subtle complexities, and this is shown by the second part of this investigation, a search for the structures of clusters beyond the dimer. How the small, net effect of combining dispersion, electrostatic interaction, and other effects evolves from the dimer to extended aggregations is a part of understanding the nature of H_2 noncovalent interactions. This is explored for this report by using the model potential for small and intermediate-sized clusters of hydrogen molecules to track the energetics of hydrogen molecule addition to clusters and to look at the local potential features of a single embedded molecule.

Calculational Approach

The first calculations performed provided one initial review of the basis set quality, these being full-CI calculations of the potential curve for H_2. These were done with the cc-pVTZ, aug-cc-pVTZ, and d-aug-cc-pVTZ bases of Dunning.[25] As shown in Table 1, the equilibrium bond length is very insensitive to basis improvements beyond that of cc-pVTZ. At either the MP2 level or at the CISD (full-CI for H_2) level, the basis set differences among equilibrium bond lengths were less than 0.001 Å. In most of the cluster calculations, the H_2 distance was then fixed at the full-CI value of 0.743 Å. Selected calculations were done where this constraint was relaxed. The MP2 calculations on $(H_2)_n$ clusters using the smallest basis, cc-pVTZ, and relaxing the H_2 bond length were performed with Spartan '02.[26]

Electrical properties were evaluated for use in the construction of the model potential, and results for the quadrupole moment and dipole polarizability are given in Table 1. SCF level values were obtained with the derivative Hartree−Fock (DHF) scheme,[27] and correlated values were obtained with a Romberg (fitting) analysis[28,29] for finite-field-gradient energy evaluations (i.e., with a sequence of ab initio energies for different chosen values of an external field gradient). The effect on electrical properties of using the d-aug-cc-pVTZ basis versus the aug-cc-pVTZ basis turned out to be very small, indicating the adequacy of the singly augmented set for these response properties. Correlation effects on the electrical properties are small. Correlation diminishes the size of the quadrupole moment by almost 10%, and a good fraction of this effect is recovered at the level of an MP2 evaluation (Table 1). The effect of correlation on the dipole polarizability is also small. It affects the dipole polarizability by less than 1%, as shown by the values in Table 1. Results for the quadrupole−quadrupole polarizability show a roughly comparable size of effect from correlation. The augmentation of the cc-pVTZ basis to the aug-cc-pVTZ basis, though, gives a difference more noticeable than the differences among correlation treatments. In particular, the dipole polarizability tensor components perpendicular to the bond axis increase by about 80% with basis set augmentation.

TABLE 2: Calculated Equilibrium Separation Distance and Well Depth of H_2-H_2

	aug-cc-pVTZ basis		d-aug-cc-pVTZ basis	
correlation level[a]	R_{com} (Å)	well depth (cm^{-1})	R_{com} (Å)	well depth (cm^{-1})
MP2	3.456	27.5	3.455	27.7
ACCD	3.436	29.4	3.435	29.7
CCD	3.437	29.4	3.435	29.8
B-ACCD	3.447	28.3	3.445	28.6
B-CCD	3.447	28.4	3.445	28.6

[a] The coupled cluster calculations are designated CC. ACCD refers to an approximate CC scheme[35] and B- means the calculation was done with Brueckner orbitals.[37]

Ab initio calculations for the dimer were performed with the correlation-consistent basis sets used for the monomer and with several levels of treating electron correlation. These levels are MP2 and several coupled cluster levels: CCD[30−34] (coupled clusters with doubles excitation operators), an approximate form designated ACCD[35] which has been found to well-reproduce corresponding CC results,[36] and a Brueckner orbital CCD evaluation[37,38] (B-CCD), that being the most complete treatment used here. Throughout, interaction energies were evaluated with the standard Boys−Bernardi counterpoise correction for basis set superposition error.[39]

Ab initio calculations for H_2-H_2 dimer once more verified that the equilibrium structure is that of T-shaped monomer orientations, something that can be associated with the optimum interaction of the permanent quadrupoles of the molecules. The interaction well depths and equilibrium separation distances for T-shaped H_2-H_2 are given in Table 2. These dimer results at all levels showed very little change from doubly augmenting the cc-pVTZ basis (d-aug) versus using the smaller aug-cc-pVTZ basis. This was also found by Diep and Johnson.[19] They also included the aug-cc-pVQZ basis in their calculations, and while potential curves in their report (Figure 2 of ref 19) show a noticeable difference between aug-cc-pVDZ and aug-cc-pVTZ, there is a much, much smaller difference between aug-cc-pVTZ and aug-cc-pVQZ. Finding no significant effect from double-augmentation, we chose to carry out calculations to find the equilibrium structures of the trimer and tetramer and to explore slices through the dimer's interaction surface with the aug-cc-

pVTZ basis. A limited set of calculations were done with the cc-pVTZ basis to make certain comparisons, as discussed later.

For the ground vibrational states of a number of clusters, simulations were performed by the diffusion quantum Monte Carlo method,[40] a nonapproximate treatment utilizing the equivalence of the differential equation for particle diffusion and the time-dependent differential Schrödinger equation. Monte Carlo (MC) techniques for numerical solution of the diffusion equation are used to simulate the solution of the modified Schrödinger equation via pseudoparticles (psips) that propagate in randomized, discrete time steps. The exact solution of the Schrödinger equation is approached with increasing number of time steps and psips and as the size of the time steps approaches zero. In the H_2-cluster calculations, a rigid body diffusion quantum Monte Carlo (RBDQMC) treatment[41−44] was used, wherein the diffusion steps include molecular translation plus rotation of each rigid molecule about its center of mass. At least 8000 psips and 189 000 time steps were used in each calculation, and the time step was short, 4.0 au (time). (1.0 au (time) or 1.0 $h/(2\pi E_h) = 2.41888 \times 10^{-17}$ s.) Calculations done for $(H_2)_2$ with a shorter time step of 2.0 au showed differences less than the statistical error limits of the corresponding 4.0 au time step calculations. While the diffusion simulation yields weights for each psip that reflect the quantum probability densities[45] at the corresponding positions of the psips, the true probability density can be obtained by descendant weighting,[46,47] and this was done for obtaining vibrational state averages of properties.

Results and Discussion

Ab Initio Results for the Dimer, Trimer, and Tetramer. The T-shaped equilibrium structure of the dimer has a separation between the molecular mass centers of 3.45 Å, and because of the overall shallowness, the potential is very flat in the vicinity of the equilibrium. The minimum energy path for internal rotation, or really for an interconversion that swaps the top of the T with the post of the T, passes through a parallel structure of C_{2h} symmetry. The optimum parallel structure has the molecules offset such that there is an attractive quadrupole−quadrupole interaction. This is generally referred to as a slipped parallel structure and it is the transition state structure for interconversion. At this structure the separation between the parallel axes of the two molecules is 2.530 Å and the offset, or slip, is 2.383 Å, according to the results of our aug-cc-pVTZ MP2 calculations. This makes for a separation between the mass centers of 3.475 Å, and that is within 0.03 Å of the separation at the T-shaped equilibrium structure. The barrier, which is the difference between the energies of the slipped parallel and the T-shaped structures, is less than 3 cm^{-1}, and hence, the interconversion path is one for which the molecules can almost freely tumble around each other with a potential that has small anisotropy. That feature is consistent with the early, common use of isotropic potentials for $(H_2)_2$ dynamical simulations. Clearly, for certain applications, that is a reasonable simplification of the interaction potential. It is important to realize for the discussion that follows that this feature, the near-isotropy of the potential along the interconversion path, has much to do with the nature of quadrupole−quadrupole interactions plus the unique juxtaposition of that effect with the nonelectrical effects among hydrogen molecules. A slightly different molecular bond length, a different quadrupole moment, or a different polarizability could undo the special balance that leads to the low barrier and the nearly constant mass center separation distance along the interconversion path.

Our ab initio calculations yielded an equilibrium structure of the trimer that is planar and cyclic (C_{3h} symmetry), with separations between monomer mass centers of 3.43 Å. The trimer's triangular structure corresponds to a compromise in the optimum arrangements of interacting quadrupoles with each pair slightly offset from a perfect T-shape in order to close the ring. The angle between a molecular H−H axis and the line from its center of mass to the next molecule's center of mass is 75°, compared to 90° for the dimer (for a T-shape).

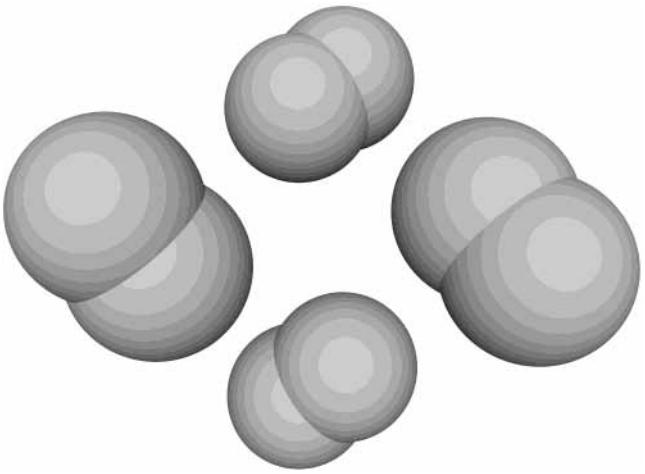

Figure 1. Equilibrium structure of $(H_2)_4$ obtained from MP2 calculations with the aug-cc-pVTZ basis and fixed monomer bond lengths. The tetramer is a near tetrahedral structure with mass centers of the monomers lying 1.161 Å above and below a symmetry plane for an S_4 symmetry operator.

A tetramer structure that perfectly preserves T-shaped arrangements for each pair of adjacent molecules can be formed as a square planar cluster (D_{4h} symmetry). Numbering the molecules 1 through 4 sequentially around the ring, we can say that the quadrupoles of the pairs of closest neighbors, that is, 1−2, 2−3, 3−4, and 4−1, can be favorably arranged. Furthermore, molecules on opposite corners (1−3 and 2−4) are parallel and offset, though not at the optimum distance of the slipped parallel dimer structure. Through out-of-plane distortion of such a structure, though, the T-shaped and slipped parallel interactions can, as an overall sum, be enhanced slightly. The molecules twist relative to one another, largely preserving the T-shaped arrangements among adjacent pairs while decreasing the distance between parallel molecules. This leads to the nonplanar equilibrium structure of $(H_2)_4$ shown in Figure 1. However, it is very important to recognize the stabilization gained from nonplanarity is quite small, with there being less than 17 cm^{-1} difference between nonplanar (fully optimized) structures and the optimum planar-constrained tetramer structures (MP2/aug-cc-pVTZ level).

As shown in Table 2, the well depth for the dimer is 28.4 cm^{-1} (40.9 K) at the B-CCD aug-cc-pVTZ level and 28.6 cm^{-1} (41.1 K) at the B-CCD d-aug-cc-pVTZ level. MP2 yields a well depth that is about 3% less deep than that obtained with B-CCD. Diep and Johnson[19] have the most complete calculational results for $(H_2)_2$, and they found a difference larger than 3% between MP2 and CCSD(T) and, more noticeably, a deeper well (near 50 K). Part of this is due to a small difference in the monomers' bond lengths between the two sets of calculations. While Diep and Johnson also used rigid H_2 molecules, their fixed H−H distance was set to 0.7668 Å to correspond to the vibrationally averaged bond length of H_2, whereas we used 0.743 Å, the equilibrium separation from the full-CI aug-cc-pVTZ calculation. These are largely elective choices, but they have an influence on detailed comparisons. In particular, a well depth will tend to be deeper when the separated limit is that of

nonequilibrium monomer structures. This is because the monomers' electronic structures can adjust in the presence of a partner molecule so as to offset being stretched, but not in the isolated limit. In other words, nonequilibrium molecules will tend to stick more than molecules kept at their equilibrium. We carried out a B-CCD calculation using monomer H−H distances of 0.7668 Å instead of 0.743 Å and did, in fact, obtain a deeper well of 29.6 cm^{-1} (42.6 K). The extrapolation to a complete basis set limit by Diep and Johnson[19] points to a basis set error in the well depth obtained with the aug-cc-pVTZ basis of 2 K, and the remainder of the difference (about 5 K) has to be associated with difference between our B-CCD correlation treatment and their use of CCSD(T). We wanted to employ a calculational level that could be used for geometry optimization for at least $(H_2)_4$ (to compare with the model potential results), not only $(H_2)_2$ surface points, and so their calculations[19] provide an extremely helpful means for assessing the lingering errors in our lower level results.

Diep and Johnson[19] made a number of comparisons at a fixed distance between the H_2 molecules of 3.4 Å, a separation close to the dimer's equilibrium for most levels of calculations. From this they argued that MP2 "seriously underestimates the attraction" and that "CCSD(T) is able to recover over 99.8% of the FCI binding." These are valid within the context of the comparison, but it is also useful to realize that potential curves from different levels of calculation may have minima at different separations. One curve may be heading upward when another is heading downward and still another is at its minimum. Energy differences among levels of treatment when done at a single geometry will tend to be greater than differences among minimum energies. We may expect these to be quite small effects, but of course, the interaction energetics of $(H_2)_2$ are also small. The FCI calculation used to compare with CCSD(T) was at the 3.4 Å separation and was with a small basis, aug-cc-pVDZ, which was shown[19] to have even greater differences relative to using aug-cc-pVTZ than the differences between MP2 and CCSD(T). Our B-CCD well depth (using 0.7668 Å for the H−H distance) of 29.6 cm^{-1} (42.6 K) can be compared to the CCSD(T) value of Diep and Johnson with the same basis, which we extract from their figures to be around 48 K (this was not a directly reported value). The rest of the difference, about 5 K, has to do with the different evaluations of the correlation energy. We note that B-CCD implicitly includes certain of the effects of all odd-order substitutions, though in an indirect manner. The triples in CCSD(T) are included perturbatively, and that can lead to small overvaluing, undervaluing, or even both at different places along a potential curve. The single FCI calculation of Diep and Johnson is an important indication, though it probably does not distinguish accuracy of the correlation treatment to the last 1 or 2 K. On the other hand, the extrapolation to the complete basis set limit in the work of Diep and Johnson seems a clear indication that there remains a small undervaluing of the well depth with the aug-cc-pVTZ basis for any correlation treatment. We conclude that MP2 relative to B-CCD (0.743 Å H−H distance and comparison of each curve's minimum) undervalues the well depth of $(H_2)_2$ by 0.9 cm^{-1} (1 K) (from values in Table 2). From the basis set extrapolation of Diep and Johnson,[19] we assume lingering basis set effects at this level might amount to a lowering of another 2 K. It is possible that lingering correlation effects could amount to an additional 4 or 5 K (2 to 3 cm^{-1}) lowering, though judgment of the precise amount might await full-CI calculations with the same basis and for the entire interaction curve. As we show later, even the maximum possible error in the MP2 well depth would correspond to a much smaller error in the zero-point stability of the dimer. Most important, treatment at the MP2 level with the au-cc-pVTZ basis seems to be of sufficient accuracy to judge the effectiveness of the model potential when comparing against MP2/aug-cc-pVTZ calculations of larger clusters. This suggests the utility of using this particular model potential with higher level ab initio calculations when greater accuracy is needed.

TABLE 3: Calculated Equilibrium Structures and Energies of Cyclic $H_2-H_2-H_2$

ab initio level[a]	R_{com} (Å)	θ (deg)[b]	interaction energy (cm^{-1})	three-body energy (cm^{-1})
MP2	3.437	75	83.1	2.6
ACCD	3.420	76	88.2	1.9
CCD	3.420	76	88.4	2.0
MP2 (d-aug-cc-pVTZ)	3.433	75	84.2	2.8
B-CCD[c]	(3.433[c])	(75[c])	85.1	2.0

[a] Except where indicated otherwise, the basis set was aug-cc-pVTZ. [b] The angle is between one molecule's H−H axis and the line from its center of mass to the center of mass of the next molecule in the planar, cyclic trimer. [c] The B-CCD value was obtained at the geometry optimized at the MP2/d-aug-cc-pVTZ level.

TABLE 4: Changes in Monomer Bond Lengths and H−H Harmonic Stretching Frequencies Due to Intermolecular Interaction in $(H_2)_n$[a]

no. of cluster molecules, n	ΔR_{HH} (Å)			$\Delta\omega_e$ (cm^{-1})		
2	0.000 07	0.000 16		−2.4	0.3	
3	< 0.000 01	< 0.000 01	0.000 02	−0.8	0.4	0.5
4	0.000 08	0.000 19	0.000 30	−6.8	−4.2	−2.7
	0.000 47			−1.0		

[a] Ab initio calculations for this table were at the MP2 cc-pVTZ level.

Values in Table 3 indicate that the trimer's stability relative to separated H_2 molecules is between 84 and 85 cm^{-1}, with 84.2 cm^{-1} being the value from MP2 with the aug-cc-pVTZ basis. Three times the pair interaction (dimer energy) at this level is a very similar value of 82.2 cm^{-1}. It is clear that the distortion away from each pair being strictly T-shaped is by an amount (15°) for which the potential changes little or is rather soft. For the tetramer, the stability of 143.2 cm^{-1} is more than 4 times the pair energy, and this reflects, in part, the contribution of quadrupole−quadrupole interactions from opposite corners (1−3 and 2−4) of the cyclic structure. Four molecules clearly provide for special stability in the aggregation of hydrogen.

A special set of calculations was performed wherein the H−H bond length was optimized rather than being held fixed. These calculations were at the MP2 level with the cc-pVTZ basis, and they serve to give an idea of the effect of clustering on the monomer structures. Table 4 gives the changes in the monomer bond lengths for clusters of two, three, and four molecules relative to the optimum bond length of an isolated H_2 molecule at the same level of calculation. In all cases, the changes in bond lengths are smaller than 0.001 Å. Also shown in Table 4 are the changes in the harmonic frequencies associated with H−H stretching. Again, the effect of clustering is small. These calculations provide a good indication that structures of at least small aggregations of hydrogen molecules can be examined and suitably modeled assuming fixed H_2 structures, which has often been done in previous potential developments. Energetic and structural effects associated with neglect of the clustering influence on the H−H bond are small.

The calculations done with the cc-pVTZ basis yield geometries that are very similar to those obtained with the augmented basis sets; however, the energetics are somewhat different. Table

TABLE 5: Basis Set Augmentation Effects

	total interaction energy (cm^{-1})[a]			
	cc-pVTZ basis	aug-cc-pVTZ basis	difference	correlation energy difference (cm^{-1})[a]
$(H_2)_2$	14.8	25.9	11.1	10.0
$(H_2)_3$	45.8	79.1	33.3	30.1
$(H_2)_4$	69.7	119.5	49.8	45.0

[a] Evaluated at the cc-pVTZ/MP2 equilibrium structures for the clusters.

5 shows the interaction energies for the optimum cc-pVTZ structures evaluated both with the cc-pVTZ basis and with the aug-cc-pVTZ. When the contributions from electron correlation are separated, these results show that a large share of the greater stabilities resulting from using the augmented basis sets are via the correlation contribution. We also know that polarization via the dipole polarizability (Table 1) will show enhancement from using the aug-cc-pVTZ basis versus the cc-pVTZ basis, but this will not be as sizable. Hence, the basis augmentation can be seen as particularly important for evaluating the dispersion contribution even though the effect on separation distances and orientations at equilibrium is not very significant.

Three-body effects were evaluated for the equilibrium trimer by subtracting the corresponding pair interaction energies, those obtained from repeating the ab initio calculations on each of the three pair components of the trimer in the usual way, all with counterpoise correction. The three-body effects for the trimer at equilibrium are attractive and amount to 2.6 cm^{-1}. Three-body polarization is attractive for the cyclic trimer, though only by about 0.5 cm^{-1} from our analysis. Another possible source of three-body interaction is dipole−dipole−dipole dispersion,[48,49] though that could provide a repulsive contribution (for three interacting sites in an equilateral triangle). Given that this small three-body interaction value of 2.6 cm^{-1} necessarily relies on the counterpoise correction, which is not bounded, we did not pursue isolating many-body energies any further, noting only that for this and three other selected trimer structures, the three-body effect of polarization was consistently correct in sign, but smaller in magnitude than the ab initio values indicated.

The Model Potential. The level of treatment selected for building a model potential was MP2 with the aug-cc-pVTZ basis. As mentioned, this implies certain lingering errors such as a well depth that may be too shallow by as much as 4−6 cm^{-1}; however, it is a level at which calculations can be easily done for the trimer and tetramer, including geometry optimizations. That means the model potential's predictions can be directly checked against a corresponding level of ab initio treatment for larger clusters. The model potential, if it proves effective, could always be redetermined with a still better $(H_2)_2$ ab initio treatment. Our aim is to obtain a potential that is almost as reliable as the underlying level of ab initio treatment for small and moderate-sized clusters and which is concise enough for use in dynamical simulations.

Calculations at the MP2 level using the aug-cc-pVTZ basis were done to generate a number of different slices of the H_2−H_2 interaction surface where orientation angles and the separation distance were varied together. Each slice was generated by prescribing certain dimer structural parameters (e.g., the separation distance and the orientational angles) for the beginning and end points of the slice. Each parameter's change for a given slice was then divided into either 5 or 10 equal steps, yielding 6 or 11 points on the slice. When points turned out to be on the close-in repulsive wall such that the interaction energy was 20 cm^{-1} or more above the dissociation limit, the points were discarded. Likewise, points at long-range where the interaction energy had diminished to less than about 1 cm^{-1} were not included. This ended up meaning that all the points had a mass center separation distance of at least 3.1 Å and not greater than 4.9 Å. Some of the slices had a common initial point, and the total number of unique surface points that were generated was 94. Matching the points along these potential slices was the basis for selecting parameters in a model potential.

The model potential used the form of the molecular mechanics for clusters (MMC) model[50] which consists of two pieces, the classical electrical interaction energy, V_{elect}, and a "6−12" site−site term, V_{6-12}, to collectively represent nonelectrical effects such as dispersion, exchange, and overlap. The electrical interaction energy of V_{elect} was evaluated using the quadrupole moment, the dipole polarizability (α), and the quadrupole polarizability (C) of H_2 as obtained at the MP2 level with the aug-cc-pVTZ basis (Table 1). Because the electrical effects are quite small, only direct (not mutual) polarization effects were included. Hence, the electrical energy, V_{elect}, consisted of the quadrupole−quadrupole permanent moment interaction plus the direct polarization via α and C due to neighboring quadupole-(s). When V_{elect} is used with more than two monomers, it implicitly includes three-body polarization effects. As stated above, in three $(H_2)_3$ structures that were tested, the three-body polarization contribution was in the direction of, though less than, the ab initio three-body effect. The form of V_{elect} with embedded property values is discussed in the Appendix. An important feature is that the potential is expressed in spatial and orientational coordinates that are relative to a laboratory-fixed coordinate system. This differs from what has most commonly been done for $(H_2)_2$ which is to work with internal coordinates: the rotational angles for the monomers relative to a line between their mass centers, a torsional angle, and a separation distance. The convenience of a laboratory axis system is in treating more than a pair of molecules, and that is an important objective of this study. For the electrical interaction, necessary tensor quantities are readily collected in a common reference system such that the field and field gradients acting on a molecule can be quickly summed, tensor element by tensor element.

The total potential is $V = V_{elect} + V_{6-12}$. The site−site term, V_{6-12}, in the model potential is based on having a small number of selected sites distributed within a H_2 molecule and a 6−12 or Lennard-Jones pair interaction between every pair of sites that are located on different molecules. The general form of this potential for a collection of molecules is

$$V_{6-12} = \sum_{A}^{\text{molecules}} \sum_{B>A}^{\text{molecules}} \sum_{i}^{A\ \text{sites}} \sum_{j}^{B\ \text{sites}} \left(\frac{d_i d_j}{r_{ij}^{12}} - \frac{c_i c_j}{r_{ij}^{6}} \right) \qquad (1)$$

The set of parameters c_i and d_i comprise the model parameters that need to be found to have a complete interaction potential. For this study, which is on homomolecular clusters, they are used in a product form in eq 1 largely for convenience. For this study, single $i-j$ parameters can be expressed from carrying out the multiplication of the parameters in the form in which they have been obtained (i.e., $C_{ij} = c_i c_j$ and $D_{ij} = d_i d_j$). However, we have found a useful amount of transferability[50,51] in the site-specific parameters (c_i and d_i) such that they can be used unchanged for interactions with different kinds of molecules. We anticipate being able to use the parameters obtained here for H_2 in studying interactions of H_2 with other molecules. More extensive functional forms have been used previously to construct model potentials for solid and gas-phase H_2, such as

TABLE 6: Model Potential Parameters for eq 1[a]

site, i position (Å)[b]	c_i (au)	d_i (au)
atom centers ± 0.3715	0	151.525
center of mass 0.0	1.651	419.03
outer sites ± 0.5715	0.879	0

[a] Energies in au are found by forming products of these parameters and dividing by distances in au following eq 1. [b] The sites for V_{6-12} are located along the H−H bond axis, and their positions are given relative to the molecule's center of mass.

those by Silvera and Goldman[52] and by Etters, Danilowicz and England.[53] More complicated forms of the nonelectrical part of the potential could be employed here, especially if the objective was to extend the model's region of accurate representation of the surface further into close-in repulsive regions; however, the computational costs of using the model would then increase and the important transferability feature would not necessarily be retained, or would not be identified as easily, with other functional forms.

The parameter values were obtained by minimizing the rms deviation of energies from the model to the ab initio values for 54 points, a subset of the total set of points. We initially started with the positions of the nuclear centers as sites, and then tests were done to see if there was significant improvement from adding sites at other locations. The full set of 94 points was used to test the fits.

Searching for optimum site locations and parameters led to the use of five sites, the positions of the atomic nuclei and of the center of mass, plus two points on the H−H axis that were 0.2 Å further from the center of mass than the nuclei. The separation of the nuclei was taken to match that in the ab initio calculations, 0.743 Å. We found that the sensitivity of the rms deviation to small adjustments of the location of the two outer sites was ignorable, provided that the c and d parameters for those sites were reoptimized for different location. We also found that certain parameters for the nonatomic sites could be kept at a value of zero with an essentially nil effect on the quality of the fit. The final form of the potential required only four parameters, and their values are given in Table 6. The rms deviation of this model potential to the 54 points was about 0.5 cm^{-1}, and for the 94 ab initio surface points it was 0.95 cm^{-1}. Given that there is a lingering error in the ab initio points due to using MP2 for the correlation treatment and to lingering basis set effects that could amount to around several cm^{-1} for the equilibrium, a fitting error less than 1 cm^{-1} seemed consistent with the overall level of accuracy. Interestingly, points close to the equilibrium yielded some of the more sizable errors, and they were in the direction of having a deeper well. While it may be fortuitous that this leaves the model potential in slightly better agreement with well depths from higher level ab initio treatments than if it exactly matched all the MP2 energies, there are possible reasons why this might naturally occur so long as the functional form of the potential is well-suited overall.

The model potential was applied to find the minimum energy structures of the trimer and the tetramer, and this was done at several stages in the search for the best parameter values. Comparison of the results from the final model potential (parameters in Table 6) with the corresponding ab initio results (Table 7) shows very good agreement, especially for the stability. In addition, the interconversion potential for the dimer was generated with the model (Figure 2), and the barrier height and transition state structure were compared with what was obtained from ab initio calculations. The model gives a barrier of 3.0 cm^{-1} and the value from ab initio calculations is 2.2 cm^{-1}. From the model potential, the coordinates of the center of mass of one molecule relative to the other being at the origin (0, 0) are (2.550 Å, 2.351 Å) with the molecular axes aligned with the y-axis. From ab initio calculations, the corresponding values (2.530 Å, 2.383 Å) are very similar, especially given that slight energy changes can correspond to sizable structural changes on this weak, very flat, interaction surface.

TABLE 7: Comparison of Model and ab Initio Results for Equilibrium Structures of $(H_2)_2$, $(H_2)_3$, and $(H_2)_4$

	ab initio: MP2/aug-cc-pVTZ		model potential	
no. of molecules in cluster	R_{com} (Å)	stability (cm^{-1})	R_{com} (Å)	stability (cm^{-1})
2	3.456	27.4	3.449	29.3
3	3.437	83.1	3.452	86.0
4	3.436	143.2	3.434	144.7
	3.582[a]	3.618[a]		
4 (planar)	3.411	124.2	3.421	130.9
	4.823	4.839		

[a] Distance between 1−3 and 2−4 monomers of the tetramer, numbering them 1 through 4 around the ring.

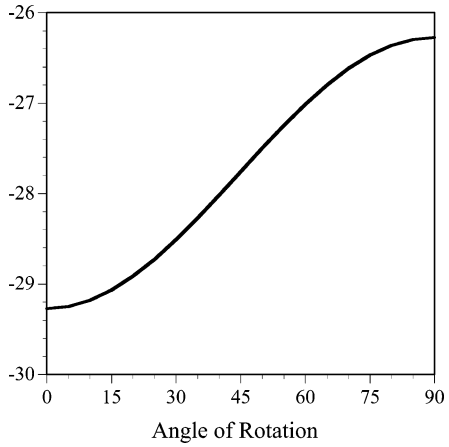

Figure 2. Interaction potential energy curve for the minimum energy path to interconvert $(H_2)_2$ from a T-shaped structure to a slipped parallel structure. The curve is from the model potential, and the coordinate used for the horizontal axis is the rotation angle of one of the molecules. The curve is symmetric about 90°. At 180°, the two H_2's have interchanged roles. The one that is the top of the T at 0° is the bottom at 180° and vice versa. The vertical axis is the model potential's interaction energy in cm^{-1}.

For the tetramer, the ab initio and model potential agree very nicely for the equilibrium energy. As well, the interaction energy of the tetramer constrained to have a planar structure is 131 cm^{-1} with the model potential and 124 cm^{-1} from the ab initio calculations.

Large Clusters of Hydrogen Molecules. The model potential facilitates studies of large clusters, and thus, calculations were performed to find the structures and stabilities of several $(H_2)_n$ clusters beyond $n = 4$, the first in this series being the pentamer. Its equilibrium structure can be described roughly as a nearly planar tetramer plus one molecule overhead to make a four-sided pyramid. A sixth molecule adds to the opposite side of the original tetramer to yield the equilibrium structure of $(H_2)_6$ according to both model calculations and MP2 cc-ppVTZ ab initio calculations. However, it is important to note that the model calculations revealed quite a number of potential minima of lower symmetry that are quite close in stability. The nearest in stability is within 10 cm^{-1} of the global minimum. A still larger number of minima were found for $n = 7$ clusters, and one had a particularly interesting arrangement of monomers. It had five equivalent hydrogen molecules in a ring. The mass centers of the hydrogen molecules in this ring were in a plane.

TABLE 8: Cluster Stabilities from Calculations with the Model Potential

no. of cluster molecules, n	equil structure stability D_e(cm^{-1})	zero-point stability D_0 (cm^{-1})	incremental energies (cm^{-1})	
			$D_e(n) - D_e(n-1)$	$D_0(n) - D_0(n-1)$
2	29.3	0.56 ± 0.04 (1.6)[a]		
3	86.0	2.09 ± 0.08 (2.2)[a]	56.7	1.53
4	144.7	4.79 ± 0.12 (12.1)[a]	58.7	2.70
5	214.1	8.63 ± 0.19	69.4	3.84
6	291.9	12.64 ± 0.25	77.8	4.01
7	374.0	17.54 ± 0.33	82.1	4.90
8	449.8	23.17 ± 0.43	75.8	5.63
9	528.1	29.74 ± 0.51	78.3	6.57
10	613.9	36.23 ± 1.51	85.8	6.49
11	708.3	43.01 ± 1.22	94.4	6.78
12	830.8	49.67 ± 1.00	122.5	6.66
13	951.1	58.18 ± 1.90	120.3	8.51

[a] Values in parentheses for $(H_2)_{2,3,4}$ are the estimates of the complete D_0 obtained from the rigid body D_0 plus one-half the change in the monomer stretch frequencies in the cluster (Table 4).

The other two hydrogen molecules were above and below the plane and over (below) the center of the ring. This structure was the model potential's global minimum energy structure of $(H_2)_7$; however, with there being other minima very close in energy, including one found to be within 10 cm^{-1}, the energetic ordering may be subject to the small errors in the model potential. While there may be a different ordering among the nearby low-energy structures than what the model potential yields, it is clear there is a high-symmetry structure among those lowest energy $(H_2)_7$ structures.

Minimum energy structures were obtained for up to 13-molecule clusters. With the number of minima increasing with cluster size, the objective was to survey the very low energy minima, especially with respect to their structural features. Searches were done from numerous initial structures. Some of these were based on adding a molecule to an optimum form of the next smaller cluster at different sites. In these cases, the geometrical parameters of the added molecule would be optimized initially with the rest of the cluster fixed. In addition, searches were made by deleting a molecule from the next larger cluster. For the $(H_2)_8$ cluster, the numerous searches repeatedly led to a small handful of lowest energy structures. We noted from these calculations that with increasing number of molecules, n, up to 8, there were an increasing number of minima close in energy to the global minimum. In other words, the global minimum was not one that was sharply distinct in energy from all the other minima as cluster size increased. Hence, for larger clusters ($n > 8$), our survey of minima offers not only a characterization of preferred structures but also provides stability information via the group of lowest energy structures. The results of many minimum energy searches for the clusters with $n > 8$ showed low-energy groupings, and the lowest energy values are reported in Table 8.

Differences in cluster energy from the nth to the $n + 1$ cluster are given in Table 8. These are a measure of the energies associated with attaching one more hydrogen molecule to a cluster of n molecules. These energies show an increase with increasing cluster size, though this is not a smoothly monotonic trend. For the $n = 12$ and $n = 13$ clusters, the incremental attachment energy of around 120 cm^{-1} is an amount that can be associated with the added H_2 being able to form at least four near T-shaped and/or near slipped parallel interactions with molecules at its optimum attachment point.

An important issue for clusters that are so weakly bound as $(H_2)_n$ clusters is the nature of their vibrational dynamics. The RBDQMC calculations show the existence of a bound state for all of the most weakly bound clusters, $(H_2)_{n=2,3,4}$. It is interesting that the zero-point energy for the dimer, though, is so sizable that the zero-point dissociation energy, D_0, is very small, about 0.6 cm^{-1}. At the same time, the sum of one-half of the harmonic vibrational frequencies of $(H_2)_2$ does not serve as an estimate of the zero-point energy because it gives a value well above the dissociation limit. We have reported a typical scaling factor for harmonic weak mode frequencies of weakly bound clusters[54] to obtain estimates of anharmonic zero-point energies, but for $(H_2)_2$, the anharmonicity effect is much, much larger than that in typical weakly bound clusters and it eclipses the scaling factor we suggested.

Reported values of the zero-point dissociation energy, D_0, of the dimer have been 3.5 cm^{-1} derived from experiment[55] and 1.58 cm^{-1} from a potential deduced from experiment.[11] The RBDQMC values of D_0 tabulated in Table 8 for $n = 2-13$ clusters are incomplete in that they are for the weak or intermolecular modes only. This is the consequence of the molecules being rigid in the RBDQMC calculations. To complete the evaluation of D_0, one must include the effects of the change in zero-point energies of the H−H stretches. From Table 4, the ab initio evaluation of the changes in the harmonic H−H stretching frequencies gives −2.4 and 0.3 cm^{-1}. Taking one-half of the sum of those differences as a good estimate of the change in zero-point energies of the monomer stretching modes; the complete D_0 for the dimer is 1.6 cm^{-1}. This value is more in the vicinity of what is accepted as a D_0 value for $(H_2)_2$ and makes the RBDQMC result of 0.56 cm^{-1} understandable.

A calculational experiment was done to examine the connection between D_0 and the well depth. Specifically, the parameters for the center of mass site of the model potential were altered slightly to lower the $(H_2)_2$ T-shaped structure's minimum energy by 1.00 cm^{-1} while keeping the optimum separation distance unchanged. This is essentially an artificial means of smoothly lowering the bottom of the well while making the smallest change to the overall potential. RBDQMC calculations were performed with this altered potential, and D_0 turned out to be more sizable but only by 0.14 cm^{-1}. In other words, a 1 cm^{-1} lowering of the well in a smooth and isotropic manner lowered the energy of the ground vibrational state by only 0.14 cm^{-1}. There is clearly a limited sensitivity of D_0 to the well depth, which is somewhat in contrast to a harmonic picture of vibration where a change in the well depth would be matched by a change in D_0. (There would be no change in *harmonic* frequencies from lowering the potential curve without changing the shape and hence no change in zero-point vibrational energies.)

It is interesting to notice the monomer contributions to D_0 for the trimer and tetramer, using the harmonic stretching

frequency changes in Table 4. While the sum of the H−H stretching frequency changes in the trimer is nearly zero, the change in the tetramer is sizable, -14.7 cm^{-1}. Combining half of this with the RBDQMC value of D_0 (for rigid H_2) yields D_0 (complete) $= 12.1$ cm^{-1} for the tetramer. It is, therefore, a significantly more stable clustering of hydrogen molecules than that of two separate dimers.

The RBDQMC values in Table 8 show that as cluster size increases, not only does D_0 increase, but the incremental amount of energy of adding another molecule increases as well, and of course, this is only the zero-point stabilities for rigid $(H_2)_n$ clusters. The zero-point stabilization per added molecule is also slowly growing from $n = 2$ to $n = 13$ as a fraction of the incremental D_e. It is important to recognize that the DQMC calculations that yield this small cluster information are extensive. The calculations for the $n = 10$ cluster required about 10^{11} evaluations of the potential. It is because of the need for so many repeated potential evaluations in simulations of this sort that our modeling objective was guided toward balancing accuracy with conciseness and computational effectiveness.

Molecules in Large Clusters. The information that can be sought from calculations on larger hydrogen clusters include the incremental binding energy, the nature of the interactions that lead to that energy, the rotational potential for an embedded molecule, and vibrational dynamics. To gain understanding of fairly large clusters, it is helpful to follow a different approach from that for studying clusters with a dozen or so molecules. This approach is to presume some translational isotropy in the approach to an infinite cluster, that is, to examine regular structures of tens and hundreds of molecules. The edge effects that might persist inside such clusters are partly offset or constrained in this manner. Calculations of this sort were carried out on a number of small clusters assuming regular shapes based on the optimum forms we obtained for the trimer, the tetramer, and the hexamer. With the model potential, geometrical parameters were optimized with constraints so that the cluster had a certain regular form, again, with a number of forms tested. Then, constraints were removed in a systematic manner and geometrical parameters were reoptimized to see which constraints held. Clusters were enlarged and the process was repeated. What was obtained should be the minimum energy structure for the inside part of a very large annealed cluster of fixed hydrogen molecules at very low temperature and pressure.

Figure 3 depicts the results of searching for regularity in large clusters of hydrogen. The structural features are that the molecules exist in planes and within each plane there are rows of parallel molecules. The molecules in one row are at 45° with respect to a line passing through their mass centers. The next row has the orientation angle at −45°. The next row after that is like the first (45°) so that a herringbone pattern develops. Adjacent planes show an offset or shift in the molecule positions, and the result is that nearby molecular mass centers are arranged as a regular tetrahedron (three in one plane and one from an adjacent plane). As can be seen in Figure 3, within a plane, each molecule is participating in four planar tetramer-like arrangements. From one plane to the next, the arrangements of nearest neighbors correspond to the slipped parallel form of the dimer. An example of the type of searching that was done to identify these structures was to let the separation between molecules in a row be one coordinate (x), the separation between rows be another (y), and the separation between planes be another (z). When these three parameters were optimized independently for a cluster of 177 hydrogen molecules, they converged to values that were within 0.001 Å of a strictly tetrahedral arrangement of mass centers, with the small deviation corresponding to the limits in the optimization search. This arrangement of mass centers is what one expects for close-packing of isotropic species (e.g., atoms or spheres), and thus, it has a lot to do with the anisotropy of the basic H_2-H_2 interaction being very small. At the same time, there is a strongly preferred orientation for each molecule, indicating there is a more complicated interaction than that of spherical species.

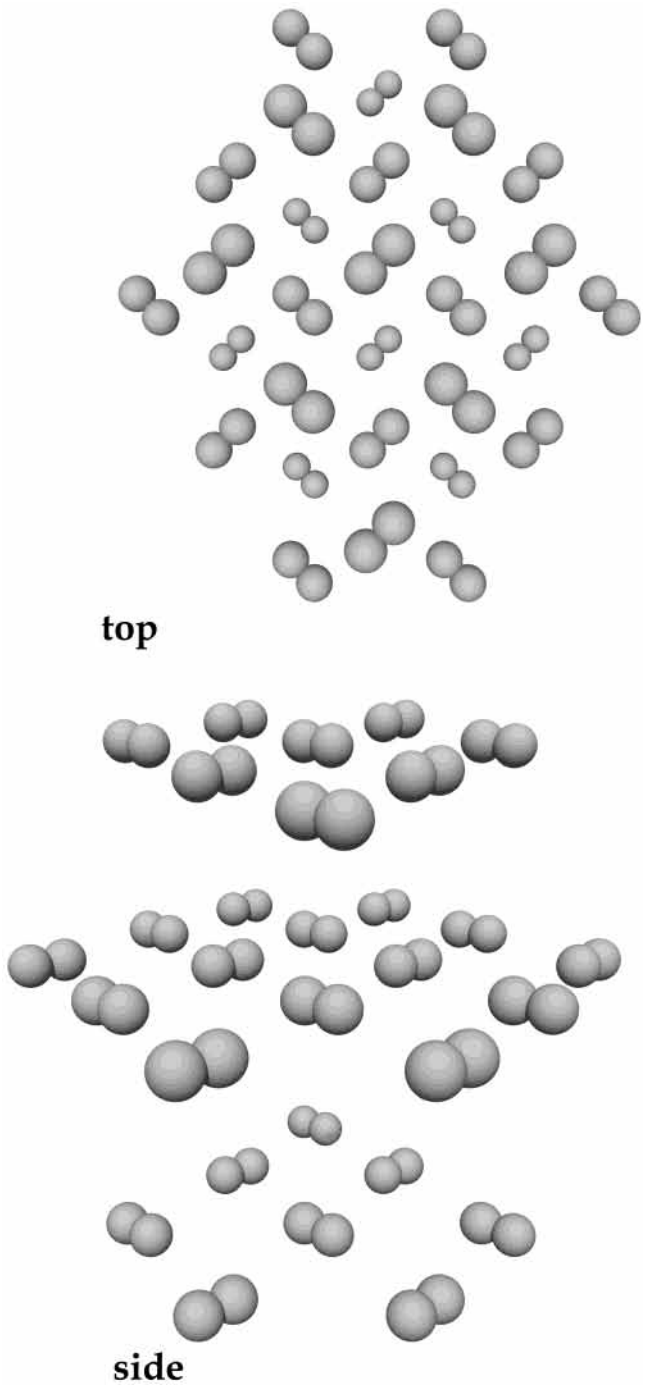

Figure 3. A regular structure of extended hydrogen molecule clusters consists of planes with the molecules in a row having parallel orientations that are ±45° twisted from the axis of the row. The top view (a) is looking into a stack of three planes, with the size of the molecules diminishing with distance from the viewer. Planar tetramer forms can be recognized by going from one molecule to the two on either side in the next row and the one between in the row following that. The side view (b) shows the closer molecules as larger than the molecules most removed from the viewer.

TABLE 9: Model Potential Results for Regular Large Clusters

no. of cluster molecules, *n*/ no. of shells	optimum molecule separation (Å)	binding energy of central H_2 (cm^{-1})
13/1	3.487	232.2
55/2	3.468	292.4
177/3	3.457	307.3
381/4	3.453	310.8

The two types of close-packing structures of spheres, hexagonal close-packing (hcp) and face-centered cubic (fcc) are both found for solid H_2, and the free energy difference seems to be small.[24,56] Calculations with the model potential for $(H_2)_{13}$ were performed with an fcc constraint and then with an hcp constraint. The cluster of 13 molecules is one in which there is a central molecule surrounded by a shell of 12 molecules in both hcp and fcc forms. The optimum separation between molecules in the two types was found to differ by only 0.0003 Å, and the stability difference was only 1.2 cm^{-1}, with the fcc form being the more stable. The difference is less than 0.2% of the cluster's stability, and with it being so small, the qualitative ordering of fcc versus hcp could be subject to small errors in the potential. What seems clear is that the model potential gives yields very little energetic and structural differentiation between fcc and hcp forms.

Calculations were performed for clusters that were "grown" according to the pattern in Figure 3 (fcc). Starting from a central molecule, a cluster was formed that included all molecules within a distance of 1.1 times the length of the side of the tetrahedron unit. This is the first shell, and it had 12 molecules. A second shell was formed by including all hydrogen molecules within 2.1 times the length of the side of the tetrahedron unit, a third shell was formed with a factor of 3.1, and a fourth shell with a factor of 4.1. There were a total of 13 molecules in the cluster with one shell around the central molecules, 55 in the cluster with 2 shells, 177 in the cluster with 3 shells, and 381 in the cluster with 4 shells. For each of these clusters, the optimum distance between molecules (edge of the tetrahedron) was obtained, and the energies of the clusters were evaluated. Then, the embedded, central molecule was removed and the energy was reevaluated. These values are shown in Table 9.

Removing the central molecule in a large cluster results in breaking the equivalent of at least 10 favorable pair interactions. Since the molecule participates in four planar tetramers, those interactions will be essentially the stabilization of the tetramer, or almost half of this binding energy. The slipped parallel interactions above and below yield the majority of the remaining interaction, and it is fair to say that each molecule has, in at least a compromised form, something close to a T-shaped or slipped parallel arrangement with each of its 12 nearest neighbors. Given that, it would seem possible for the rotation of a single H_2 in a large cluster to be hindered by its strong, multiple neighbor interaction. In fact, this does turn out to be the case in one sense. If a single hydrogen molecule is rotated so as to interchange the atoms of the molecule, the barrier for rotation is at least 60 cm^{-1}. However, through further calculations that were performed for this interconversion pathway in the 177-molecule cluster, we find that if the orientations of the nearest neighbor molecules (the surrounding shell of 12 molecules) are relaxed throughout the molecule's rotation, the barrier is reduced (for the 177-molecule) cluster to only 0.2 cm^{-1}. In other words, the nearly free rotation of a H_2 in a large aggregation comes about through a concerted rotation of the surrounding shell of nearby molecules. The distortions of the orientations of these surrounding molecules from their equilibrium orientations accommodates the rotation of the central molecule and yet are small enough to maintain most of their interaction with the hydrogen molecules in the next surrounding shell.

Conclusions

We show that a concise model potential for application to small and large clusters of hydrogen molecules can be constructed and achieve a good match to dimer, trimer, and tetramer potential surface features with only four adjustable parameters. This was done on the basis of a modest level of ab initio treatment, MP2 with the aug-cc-pVTZ basis, and it should be as effective to start with higher level ab initio treatments if higher accuracy is called for.

Hydrogen molecules interact with one another via quadrupole−quadrupole interactions, dispersion, and other repulsive and attractive elements. The net combination of effects leads to a T-shaped equilibrium structure for the dimer and a small barrier to interconversion, a process that proceeds through a slipped parallel transition state structure. In turn, there is particular stability in the four-membered cluster where there are both T-shaped and slipped parallel interactions. Our RB-DQMC calculations show that the incremental change in D_0 stability from the timer to the tetramer is a significant increase over the step from the dimer to the trimer. The preference for this structure, even in a slightly less stable planar form, can be seen in the preferred regularity of larger clusters which were examined with the model potential. The attachment energy of a molecule to a growing, large cluster was calculated to be around 300 cm^{-1} because arrangements exist whereby a H_2 molecule can interact with most all of its 12 nearest neighbors in nearly a T-shaped or else slipped parallel form. Furthermore, the internal rotation potential of an embedded molecule has a lower barrier than the interconversion of the dimer despite the numerous interacting partners that would seem to lock it in place. The model calculations show that, in part, this is because of the ease for compensating adjustments in the orientations of the nearest neighbor hydrogen molecules as the embedded molecule rotates.

Acknowledgment. This work was supported, in part, by a Grant from the Physical Chemistry Program of the National Science Foundation (CHE-0131932).

Appendix: Electrical Interaction Potential

The potential term V_{elect} is special because it has no adjustable parameters and because it has been constructed to be usable for clusters with more than two molecules. It includes direct, not back, polarization, and in that, brings one type of three-body term into the potential. V_{elect} is specified in terms of position coordinates (x, y, z) of the mass centers of the hydrogen molecules in a laboratory-fixed system of axes. The molecular center of mass is the reference point for the prerequisite step of ab initio evaluation of the electrical response properties. V_{elect} is also specified in terms of Euler angles for each of the interacting molecules. These correspond to a sequence of rotations: (1) rotation about the *z*-axis, (2) rotation about the *y*-axis, and (3) rotation about the *z*-axis. The electrical potential experienced by a molecule is found by summing contributions from all other molecules using the laboratory axis system. This is advantageous because the same transformation of property tensors is used for all pairs, whereas with a local (pair) axis system, such tensor transformations would be performed over

and over. The electrical interaction energy of a molecule is evaluated as both the interaction of the quadrupole and the polarization energy via the dipole and quadrupole polarizabilities. The electrical potential as part of the total potential for $(H_2)_n$ reported here is available as a downloadable FORTRAN source code.[57]

References and Notes

(1) *National Hydrogen Energy Road map*; USDOE: Washington, DC, 2002.

(2) Hixson, H. G.; Wojcik, M. J.; Devlin, M. S., Devlin, J. P.; Buch, V. *J. Chem. Phys.* **1992**, *97*, 753.

(3) Buch, V.; Devlin, J. P. *J. Chem. Phys.* **1993**, *98*, 4195.

(4) Buch, V.; Silva, S. C.; Devlin, J. P. *J. Chem. Phys.* **1993**, *99*, 2265.

(5) Vos, W. L.; Finger, L. W.; Hemley, R. J.; Mao, H. *Phys. Rev. Lett.* **1993**, *71*, 3150.

(6) Li, J.; Furuta, T.; Goto, H.; Ohashi, T.; Fujiwara, Y.; Yip, S. *J. Chem. Phys.* **2003**, *119*, 2376.

(7) Gordon, R. G.; Cashion, J. K. *J. Chem. Phys.* **1966**, *44*, 1190.

(8) Farrar, J. M.; Lee, Y. T. *J. Chem. Phys.* **1972**, *57*, 5492.

(9) Dondi, M. G.; Valbusa, U.; Scoles, G. *Chem. Phys. Lett.* **1972**, *17*, 137.

(10) Monchick, L. *Chem. Phys. Lett.* **1974**, *24*, 91.

(11) Gengenbach, R.; Hahn, C.; Schrader, W.; Toennies, J. P. *Theor. Chim. Acta* **1974**, *34*, 199.

(12) Bauer, W.; Lantzsch, B.; Toennies, J. P.; Walaschewski, K. *Chem. Phys.* **1976**, *17*, 19.

(13) England, W.; Etters, R. D. *Mol. Phys.* **1976**, *32*, 857.

(14) Gallup, G. A. *J. Chem. Phys.* **1977**, *66*, 2252.

(15) Schaefer, J.; Meyer, W. *J. Chem. Phys.* **1979**, *70*, 344.

(16) Schaefer, J.; Watts, R. O. *Mol. Phys.* **1982**, *47*, 933.

(17) Burton, P. G.; Senff, U. E. *J. Chem. Phys.* **1982**, *76*, 6073.

(18) Wind, P.; Roeggen, I. *Chem. Phys.* **1992**, *167*, 263; **1993**, *174*, 345; **1996**, *211*, 179.

(19) Diep, P.; Johnson, J. K. *J. Chem. Phys.* **2000**, *112*, 4465.

(20) Bender, C. F.; Schaefer, H. F. *J. Chem. Phys.* **1972**, *57*, 217.

(21) (a) McLaughlin, D. R.; Schaefer, H. F. *Chem. Phys. Lett.* **1971**, *12*, 244. (b) Schaefer, H. F. *The Electronic Structure of Atoms and Molecules*; Addison-Wesley: Reading, MA, 1972.

(22) McKellar, A. R. W. *Astrophys. J.* **1988**, *326*, L75.

(23) McKellar, A. R. W.; Schaefer, J. *J. Chem. Phys.* **1991**, *95*, 3081.

(24) Silvera, I. F. *Rev. Mod. Phys.* **1980**, *52*, 393.

(25) Dunning, T. H. *J. Chem. Phys.* **1989**, *90*, 1007.

(26) *Spartan '02*, version 1.0.4e. Wave Function Inc.: Irvine, CA, 2002.

(27) Dykstra, C. E.; Jasien, P. G. *Chem. Phys. Lett.* **1984**, *109*, 388.

(28) Champagne, B.; Mosley, D. H. *J. Chem. Phys.* **1996**, *105*, 3592.

(29) A FORTRAN program for Romberg analysis may be downloaded from: http://www.chem.iupui.edu/faculty/images/Romberg_fitting_program-.html.

(30) Cizek, J. *Adv. Chem. Phys.* **1968**, *14*, 35.

(31) Cizek, J.; Paldus, J. *Int. J. Quantum Chem.* **1971**, *5*, 359.

(32) Bartlett, R. J.; Purvis, G. D. *Int. J. Quantum Chem.* **1978**, *14*, 561; *Phys. Scr.* **1980**, *21*, 255.

(33) Nakatsuji, N.; Hirao, K. *J. Chem. Phys.* **1978**, *68*, 2053.

(34) Pople, J. A.; Krishnan, R.; Schlegel, H. B.; Binkley, J. S. *Int. J. Quantum Chem.* **1978**, *14*, 545.

(35) (a) Jankowski, K.; Paldus, J. *Int. J. Quantum Chem.* **1980**, *18*, 1243. (b) Chiles, R. A.; Dykstra, C. E. *Chem. Phys. Lett.* **1981**, *80*, 69.

(36) (a) Dykstra, C. E.; Liu, S.-Y.; Daskalakis, M. F.; Lucia, J. P.; Takahashi, M. *Chem. Phys. Lett.* **1987**, *137*, 266. (b) Dykstra, C. E.; Davidson, E. R. *Int. J. Quantum Chem.* **2000**, *78*, 226.

(37) Chiles, R. A.; Dykstra, C. E. *J. Chem. Phys.* **1981**, *74*, 4544.

(38) Handy, N. C.; Pople, J. A.; Head-Gordon, M.; Raghavachari, K.; Trucks, G. W. *Chem. Phys. Lett.* **1989**, *164*, 185.

(39) Boys, S. F.; Bernardi, F. *Mol. Phys.* **1970**, *19*, 553.

(40) Anderson, J. B. *J. Chem. Phys.* **1975**, *63*, 1499.

(41) Buch, V. *J. Chem. Phys.* **1992**, *97*, 726.

(42) Franken, K. A.; Dykstra, C. E. *J. Chem. Phys.* **1994**, *100*, 2865.

(43) Gregory, J. K.; Clary, D. C. *Chem. Phys. Lett.* **1994**, *228*, 547.

(44) Dykstra, C. E.; Van Voorhis, T. A. *J. Comput. Chem.* **1997**, *18*, 702.

(45) Reynolds, P. J. *J. Chem. Phys.* **1990**, *92*, 2118.

(46) Coker, D. F.; Watts, R. O. *J. Phys. Chem.* **1987**, *91*, 2513.

(47) Kalos, M. H. *Phys. Rev. A* **1970**, *2*, 250.

(48) Axilrod, B. M.; Teller, E. *J. Chem. Phys.* **1943**, *11*, 299.

(49) Thakkar, A. J. Intermolecular Interactions. In *Encyclopedia of Chemical Physics and Physical Chemistry*; IOP Publishing: Bristol, U.K., 2000.

(50) Dykstra, C. E. *J. Am. Chem. Soc.* **1989**, *111*, 6168.

(51) Dykstra, C. E. *Adv. Chem. Phys.* **2003**, *126*, 1.

(52) Silvera, I. F.; Goldman, V. V. *J. Chem. Phys.* **1978**, *69*, 4209.

(53) Etters, R. D.; Danilowicz, R.; England, W. *Phys. Rev. A* **1975**, *12*, 2199.

(54) Dykstra, C. E.; Shuler, K.; Young, R. A.; Bacic, Z. *J. Mol. Struct. (THEOCHEM)* **2002**, *591*, 11.

(55) Watanabe, A.; Welsh, H. L. *Phys. Rev. Lett.* **1964**, *13*, 810.

(56) Collins, G. W.; Unites, W. G.; Mapoles, E. R.; Bernat, T. P. *Phys. Rev. B* **1996**, *53*, 102.

(57) A FORTRAN program for the model potential may be downloaded from: http://www.chem.iupui.edu/faculty/images/hydrogen_clusters.html.